

# New technique for the fabrication of miniature thin film heat flux gauges

Matthew Collins, Kam Chana and Thomas Povey

Osney Thermofluids Laboratory, Department of Engineering Science, University of Oxford, Parks Road, Oxford, OX1 3PJ, UK

Email: [matthew.collins@eng.ox.ac.uk](mailto:matthew.collins@eng.ox.ac.uk), [kam.chana@eng.ox.ac.uk](mailto:kam.chana@eng.ox.ac.uk) and [thomas.povey@eng.ox.ac.uk](mailto:thomas.povey@eng.ox.ac.uk)

Received 25 July 2014, revised 5 November 2014

Accepted for publication 2 December 2014

Published 20 January 2015



## Abstract

This paper details the improvements made to the design and fabrication of thin-film heat flux gauges at Oxford. These improvements have been driven by the desire to improve measurement accuracy and resolution in short duration wind-tunnel experiments.

A thin-film heat flux gauge (TFHFG) measures heat flux by recording the temperature history of thin film resistive temperature sensors sputtered onto an insulating substrate. The heat flux can then be calculated using Fourier's law of heat conduction.

A new fabrication process utilising technology from the manufacture of flexible printed circuit boards is outlined, which enables the production of significantly smaller and more robust gauges than those previously used.

Keywords: thin film gauges, heat flux gauges, heat transfer

(Some figures may appear in colour only in the online journal)

## Nomenclature

$\alpha$	Temperature coefficient of resistance
$C$	Rotor true chord (OTRF = 36.6 mm)
$c$	Specific heat
$d$	TFHFG platinum sensor thickness
$D$	Thermal diffusivity $\lambda / \rho c$
$h$	Heat transfer coefficient ( <i>HTC</i> )
$I$	Excitation current
$\lambda$	Thermal conductivity
$L$	TFHFG platinum sensor length
$Nu$	Nusselt number: $hC / \lambda_{01}$
$p$	Pressure
$\rho$	Density
$\rho_e$	Material resistivity
$\dot{q}$	Heat flux
$t$	Time
$T$	Temperature
$\bar{T}$	Time mean temperature
$V$	Voltage
$W$	TFHFG platinum sensor width

$x$  Depth from surface

## Subscripts

01	Inlet total
$AW$	Adiabatic wall
$W$	Wall

## 1. Introduction

The thin film heat flux gauge was first used to record heat transfer within a shock tunnel [1]. The TFHFG was extensively developed at the Osney Laboratory, the history of which is described by Jones [2, 3]. They are fabricated by sputtering a thin layer of platinum ( $<0.04\mu\text{m}$ ) onto a polyimide substrate with copper tracks forming the connections.

### 1.1. Principle of operation

The TFHFG (figure 1) operates on the principle that the heat flux into a surface can be calculated by measuring or calculating the temperature gradient within a material of known thermal properties using Fourier's law

$$\dot{q} = -\lambda \nabla T \quad (1)$$

Content from this work may be used under the terms of the Creative Commons Attribution 3.0 licence. Any further distribution of this work must maintain attribution to the author(s) and the title of the work, journal citation and DOI.

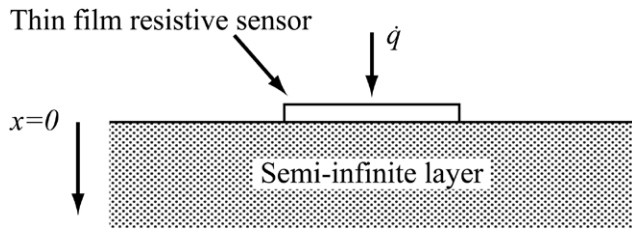


Figure 1. Single layer TFHFG.

The theory can be extended to an unsteady problem whereby the surface temperature history of a material can be used to calculate the heat flux by applying the heat-conduction equation

$$\frac{\partial^2 T}{\partial x^2} = \frac{1}{D} \frac{\partial T}{\partial t} \quad (2)$$

These equations can be solved analytically in the discrete time domain for a limited set of boundary conditions and the data processed numerically [4, 5]. Alternatively the data can be processed using a computationally more efficient impulse response method [6].

There are two principal types of TFHFGs, single layered gauges and double layered gauges. A single layered gauge comprises of one thin film resistive sensor on an insulating substrate. Most commonly the substrate is thick enough such that for the experiments duration it is considered semi-infinite in depth. However Oldfield [6] describes impulse response methods which can process data from gauges located on two layered substrates and those on an insulating layer atop an isothermal surface. These gauges are used when it is possible to assume isothermal conditions in a sufficiently thick insulating substrate at the start of the measurement.

### 1.2. Conventional design and fabrication techniques

TFHFGs were first manufactured on ceramic substrates (or enamelled metal parts) using a firing process [4]. The resistive element is typically platinum, though nickel has also been used. The resistive sensor is connected via tracks of gold or copper to points at which wiring can be soldered. The platinum resistive sensor and copper tracks are painted on using a metallo-organic ink. The sample is then fired to leave behind conducting platinum and copper tracks. This method is still used in high temperature applications which are not subjected to large mechanical stresses. This technique is very labour intensive and the size of the sensors is usually quite large (typically  $3000 \times 300 \mu\text{m}$ ).

The above method was improved upon by Thorpe *et al* [7]. Rather than hand painting each gauge, the entire substrate is covered in a fired layer of metallo-organic ink. A laser is then used to ablate the unwanted conducting film to leave the desired gauges. With this method, gauges of dimensions of  $1000 \times 80 \mu\text{m}$  can be produced. The spatial resolution of this method is typically limited by the width of the gold/copper connecting tracks which are typically quite thin ( $<0.5 \mu\text{m}$ ). This method also requires a substantial amount of time and care to set up and program the laser when used on 3D surfaces.

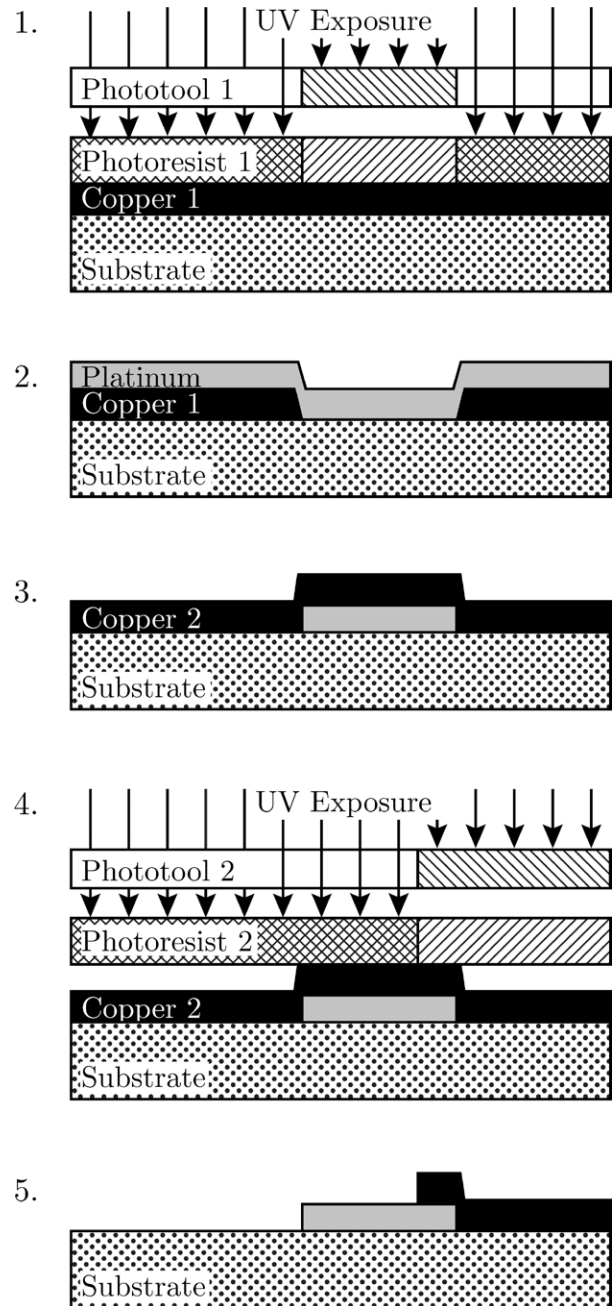
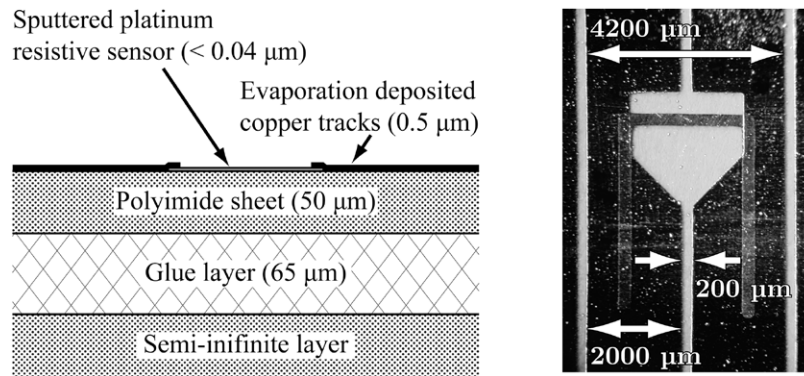


Figure 2. Conventional gauge manufacturing process.

Another approach, developed by Epstein *et al* [8] and used extensively in Oxford since, is to manufacture TFHFGs on a flexible polyimide substrate. These flexible gauges can then be laminated to the test piece using a glue layer [11]. The process utilises photolithography techniques which can create intricate features. The process can also be used to manufacture large volumes of gauges as the technique requires substantially fewer man hours than the firing processes.

From now on these flexible TFHFGs are referred to as the ‘conventional’ type. This process has been used to manufacture TFHFGs at a number of institutions since. Many published TFHFG designs are similar to those used at Oxford with a linear platinum sensor, for example those used on the turbine instrumented by Anthony *et al* [9]. Ohio State



**Figure 3.** Conventional TFHFG typical dimensions.

manufacture a TFHFG with a different design consisting of a nickel serpentine sensor with dimensions of  $1.3 \times 1.0$  mm [10]. A 4-wire measurement technique is used which requires 4 measurement leads per gauge, this increases the minimum gauge spacing to approximately 3 mm.

The fabrication process subsequently developed at Oxford consists of sputtering a thin layer of platinum ( $<0.04 \mu\text{m}$ ) onto a polyimide substrate. Copper tracks are then deposited in a vacuum chamber by evaporation to a thickness of  $0.5 \mu\text{m}$ . The process used at the Osney laboratory for a number of years has not been fully described in published literature and is illustrated in figure 2 and outlined below

1. Sputter polyimide surface with a layer of copper. Apply photoresist, overlay phototool 1, expose and develop.
2. Etch copper, remove developed phototool and sputter a layer of platinum.
3. Etch away the copper underneath the unwanted platinum, leaving the platinum sensing elements. Deposit a new layer of copper over entire surface.
4. Apply photoresist, overlay phototool 2 and expose.
5. Etch away unwanted copper then remove developed phototool to leave completed gauges.

This process is reasonably time consuming and the copper tracks are fragile, typically cracking and lifting off when bent around small radii. This imposes a limit of  $0.5 \mu\text{m}$  on the thickness of the copper tracks for typical applications. To ensure that their resistance and corresponding thermal resistance changes during an experiment are negligible the copper tracks must be made relatively wide ( $2000 \mu\text{m}$ ).

Figure 3 shows the design of a typical conventional gauge manufactured using a  $200 \mu\text{m}$  processing resolution. The platinum sensing element is  $2000 \times 200 \mu\text{m}$  giving a  $L/W$  ratio of 10. The lateral gauge spacing is 4.4 mm.

## 2. New manufacturing technique

The size of conventional TFHFGs is limited by the width of the copper connecting tracks. The tracks can be made narrower either by making them thicker or by moving to a four wire measurement system, with separate exciting and sensing tracks. The four wire approach is undesirable as it increases

the complexity and number of connections, though the principle has been used to fabricate small high density TFHFG arrays [12].

Since the manufacturing process of conventional TFHFGs was developed in the early 1990s at Oxford, there has been a huge increase in the development and manufacturing of flexible printed circuits (FPCs). These circuits are manufactured by etching a pre-laminated sheet of copper and polyimide using a dry film photoresist. These pre-laminated materials are available without an adhesive between the copper and polyimide layer. The copper quality is such that the sheets can be repeatedly folded without delamination, despite having a copper thickness that can be in the hundreds of microns.

### 2.1. Manufacturing process

To make use of a pre laminated copper-polyimide laminate, a new manufacturing process has been devised. The metal lift off process previously used to fabricate the platinum sensors is replaced with a dry film photoresist lift off technique as described by Chew *et al* [13]. The platinum film is now deposited over pre-etched copper tracks, manufactured in a dedicated FPC fabrication facility using the process illustrated in figure 4 and outlined below.

1. Apply photoresist, overlay phototool 1, expose and develop.
2. Etch copper then remove developed photoresist.
3. Apply new photoresist, overlay phototool 2, expose and develop.
4. Sputter entire surface with platinum.
5. Remove developed photoresist taking away unwanted platinum.

Using this process, TFHFGs (figure 5) have been manufactured with the use of  $18 \mu\text{m}$  thick copper connecting tracks (36 times thicker than conventional gauges). This permits connecting track widths of  $100 \mu\text{m}$ , the fine line resolution of the etching process. This has substantially improved the achievable TFHFG density, now primarily limited by the footprint of the platinum sensor element rather than the connecting tracks. The new gauges have also proven to be much more resistant to bending and abrasion, easing installation and extending operating life.



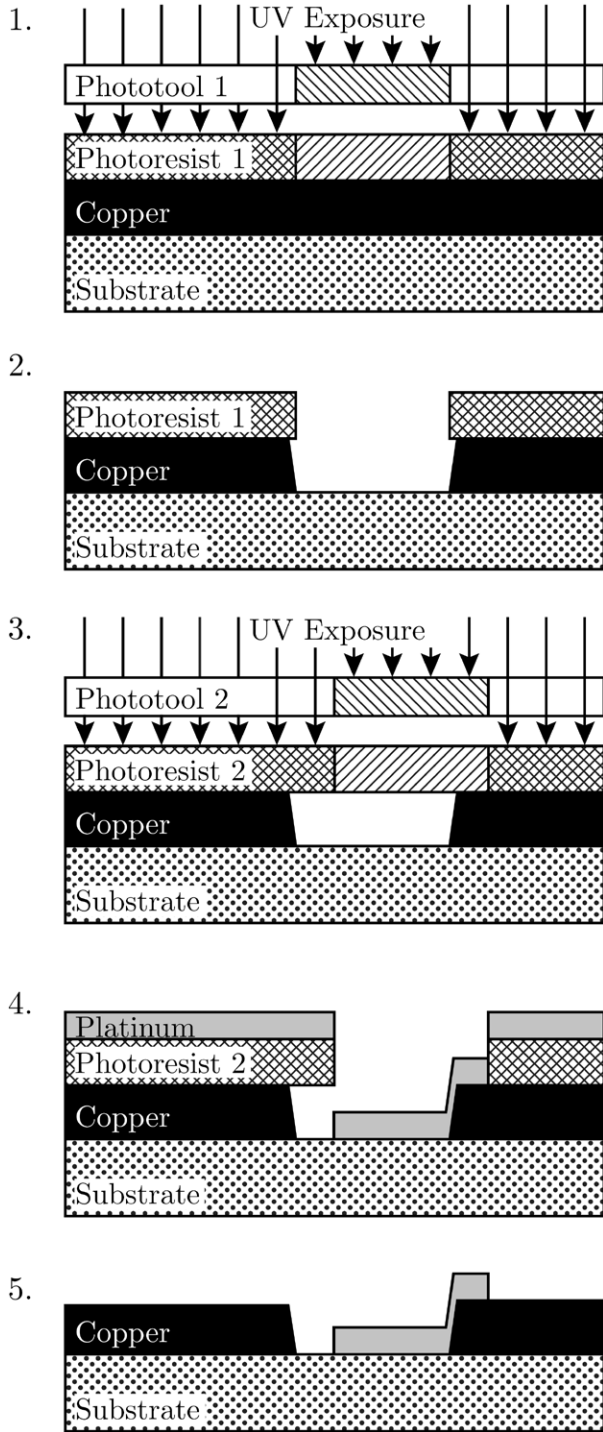


**Figure 4.** New TFHFG manufacturing process.

## 2.2. SEM analysis

The new manufacturing process relies on a good bond being formed between the etched copper connecting tracks and the deposited platinum film. A scanning electron microscope (SEM) was used to image the interface, as shown in figure 6.

A good copper/platinum bond is evident along a substantial portion of the interface with a platinum meniscus formed. In places, cracks are visible along the interface. This is most likely due to differing thermal expansion of the copper and polyimide during platinum deposition or during calibration.

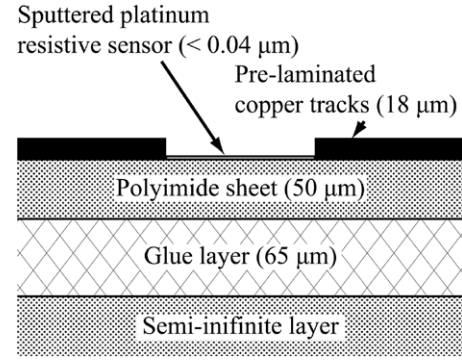


**Figure 5.** New TFHFG typical dimensions.

The flaws signify the importance of maximising the length of the copper/platinum interface, which in this case is achieved by utilising a long thin connecting copper track at the interface.

Also visible in the SEM images is the porous nature of the deposited platinum. It is not clear what causes this porosity, but it could be due to the interaction between the deposited film and the surface topology of the polyimide substrate, as visible in figure 7. During the laminates manufacture, the polyimides surface is roughened using an oxygen plasma as described by Yang *et al* [14], before bonding with copper. It is this roughness, of comparable length scale to the platinum's porosity, that is visible in figure 7.

## 2.3. Optimized design of gauges

The parameter of most interest to the thin film gauge designer is the magnitude of the voltage signal generated across the element relative to the change in temperature.

$$\frac{\Delta V}{\Delta T} = I (\alpha_{Pt} R_{0,Gauge} + \alpha_{Cu} R_{0,Track}) \quad (3)$$

The platinum element will also generate heat due to resistive heating by the excitation current. This heat will be dissipated by 1D conduction and convection but must be small enough to not affect the measurement.

$$\dot{q}_{internal} = \frac{I^2 \rho_e}{d} \quad (4)$$

These equations can be combined with the resistance defined in terms of the geometry to give an equation for the gauge sensitivity. Assuming that changes in the connecting track resistance are negligible

$$\frac{\Delta V}{\Delta T} = \alpha_{Pt} \frac{L}{W} \sqrt{\frac{\dot{q}_{internal} \rho_e}{d}} \quad (5)$$

The internal heat flux generation of the gauge is limited to an experimentally determined value which results in no measurable heating of the gauge. Sensitivity can then be increased by maximising the  $L/W$  ratio and reducing the platinum thickness (though this is the less dominant term). Using a material with a larger  $\alpha$  value will also improve the sensitivity, however platinum is typically the material of choice due to the

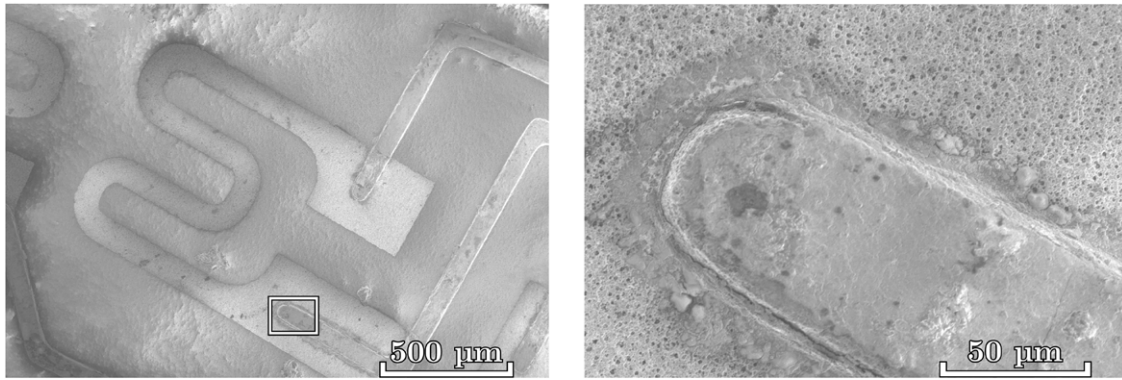


**Figure 6.** SEM images of TFHFG manufactured using the new process.

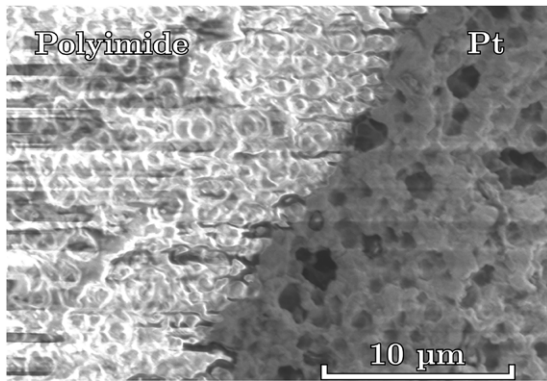


**Figure 7.** SEM image of platinum deposited on polyimide substrate.

consistency of  $\alpha$  over a large temperature range which significantly eases calibration.

Previous TFHFGs in use at Oxford utilise a linear platinum sensor element with  $L/W$  of 10. This design originated from the use of hand painted platinum sensors on ceramic and glass which were developed in the 1960s [4]. New gauge designs have been created which maximise the  $L/W$  ratio for a given gauge footprint and are shown in figure 8. Features were rounded to improve the structural rigidity of the photoresist layer during manufacture.

Figure 9 compares the new Oxford gauge to conventional gauges produced at Oxford and also to the laser ablated gauges utilised by Thorpe *et al* [7], which have hitherto had the highest published resolution. The new TFHFG designs published here offer a 7 fold improvement in gauge density versus the conventional Oxford gauges and greater than double the resolution of the laser ablated gauges. The new Oxford gauges can offer even greater improvements in resolution for applications where the number of gauges is constrained by the total width of the connecting tracks, due to the increased connecting track thickness ( $18\mu\text{m}$  versus  $0.5\mu\text{m}$ ).

### 3. Calibration of conventional and new gauges

#### 3.1. Theory

The surface temperature of a TFHFG is measured by applying a constant current and recording the voltage across the sensor. Typically the temperature history is recorded by measuring

the initial voltage ( $V_1$ ) at a known isothermal condition ( $T_1$ ) and then recording the change in voltage

$$T_W - T_1 = \frac{V - V_1(1 + \alpha(T_1 - T_0))}{\alpha V_1} \quad (6)$$

This removes the need to measure the connecting lead resistances or the current during the run. The assumption is that the resistance of the connecting tracks and leads between the calibration and experiment are kept similar. The only parameter for each gauge that need then be calibrated is  $\alpha$ . This is calibrated by measuring the resistance using a digital multimeter (DMM) at a number of known temperatures then applying a linear regression to fit the following equation

$$R - R_0 = \alpha R_0 (T_W - T_0) \quad (7)$$

The term  $R_0$  is taken to be the resistance at  $T_0$  which is typically taken to be  $0^\circ\text{C}$  and includes the lead resistances. Thus  $\alpha$ , which is a non-dimensionalised resistance/temperature gradient, incorporates the lead resistances into its definition and is given by

$$\alpha = \frac{1}{R_0} \frac{dR}{dT} \quad (8)$$

If the lead resistances cannot be kept constant from calibration to experiment then a 4 wire measurement approach can be used. This doubles the number of connecting leads which is undesirable, unless a TFHFG array as described by Anthony *et al* [12] is used. The array approach is less robust as the failure of one TFHFG can cause failure of the entire instrumented region.

Alternatively changes in lead resistances can be corrected for by measuring the resistance of the gauge at a known temperature  $T_{\text{Gauge}}$  when installed in the experiment with a DMM. The  $\alpha$  (for use in equation (6)) can then be corrected as follows, where  $T_{\text{Gauge}}$  is the temperature of the gauge in degrees Celsius.

$$\alpha_{\text{Exp}} = \frac{\alpha_{\text{Cal}} R_{0,\text{Cal}}}{R_{\text{Gauge}} - \alpha_{\text{Cal}} R_{0,\text{Cal}} T_{\text{Gauge}}} \quad (9)$$

To convert the measured surface temperature history to heat flux requires knowledge of the thermal properties of the substrate as described by Oldfield [6]. Piccini *et al* [15] describes the calibration of  $D$  and  $\lambda$  using a shuttered hot air gun to

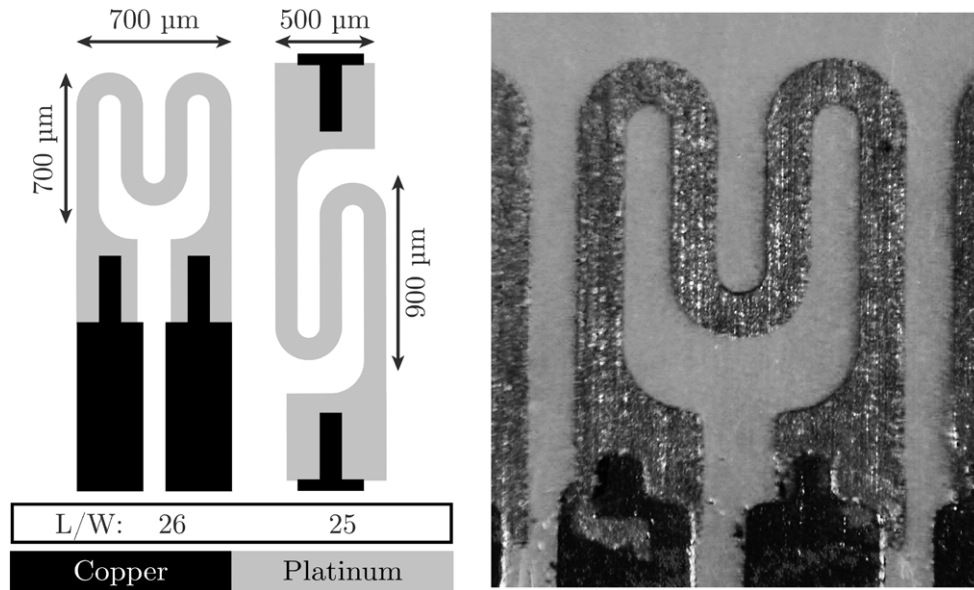


**Figure 8.** New Oxford TFHFG typical dimensions based on  $100\mu\text{m}$  processing resolution (left) and as manufactured (right).

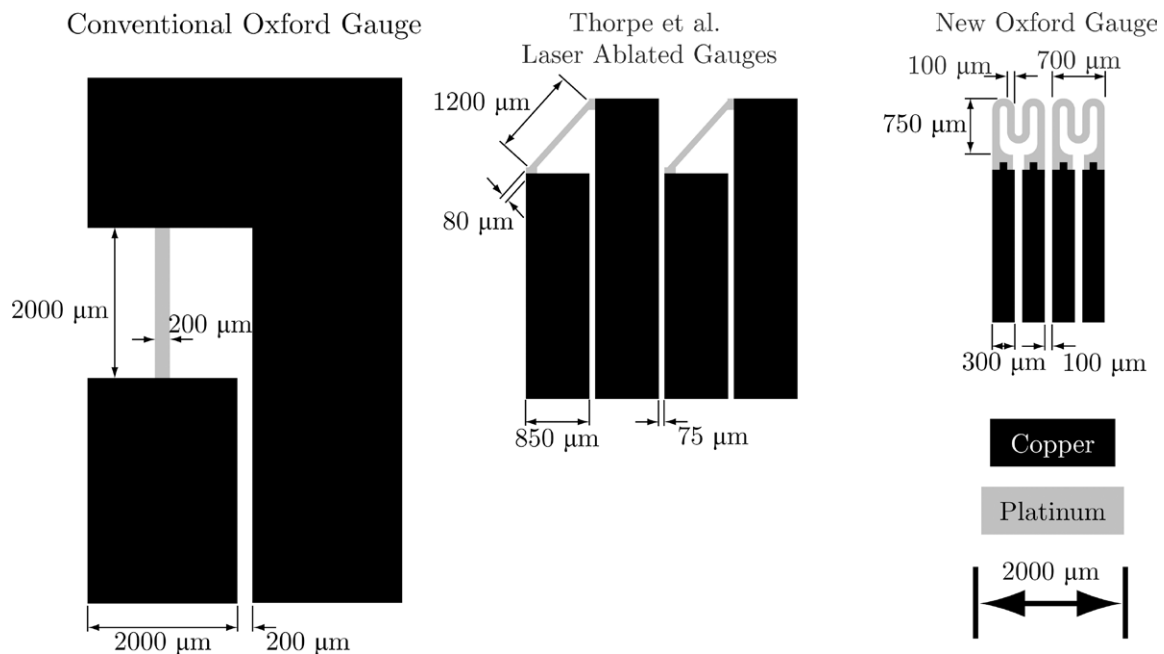


**Figure 9.** Comparison of gauge manufacturing technologies, conventional Oxford (left), Thorpe *et al* [7] laser ablated gauges (centre) and new Oxford gauge (right).

generate a step in surface heat flux, calibrated values are given in table 1. It was found that the polyimide and glue layers were found to have indistinguishable thermal properties, to the extent that they can be regarded as being the same. The new TFHFGs are manufactured on the same polyimide substrate as that calibrated by Piccini *et al* [15] and these values were retained for use with the new gauges.

### 3.2. Calibration method

TFHFGs are calibrated using a new calibration facility at Oxford. This is a National Instruments based PXI system consisting of a thermostatically controlled water bath interfaced

to a computer via a serial interface. Resistance measurements are made using a 22 bit National Instruments DMM interfaced with a relay switch module, permitting the calibration of 96 TFHFGs simultaneously. The calibration is automated and controlled with a Labview script.

The TFHFGs are calibrated when mounted to the test piece using the same wiring as when installed in the experimental facility to minimise changes in lead resistances. The test piece is instrumented with thermocouples and placed inside a plastic bag to keep it dry. Resistances are recorded at a set number of temperature steps, with test piece and water bath thermocouples monitored to ensure isothermal conditions are attained at each step.



**Table 1.** Calibrated material properties measured by Piccini *et al* [15].

Substrate	$D$	$\lambda$	$\sqrt{\rho c \lambda}$
Polyimide	$1.190 \times 10^{-7}$	0.169	490

TFHFGs are sometimes experience a drift in the value of  $R_0$  when subjected to sustained elevated temperatures. This is most likely due to stress relaxation in the platinum film and/or at the copper platinum interface. The prevalence of this effect can be reduced by depositing a thicker platinum film during the manufacturing process. Running an annealing cycle at a temperature above the calibration temperature range can also often assist with reducing this effect. The effect is observed to occur over time periods much longer than those of the experiment, so is only a problem for the calibration. As the  $\alpha$  of platinum is varies very little with temperature, the TFHFGs are typically calibrated over a lower temperature range than those experienced during an experiment. The use of a water bath incorporating a chiller assists with this. The calibration calculations can also be modified to reduce the impact of this effect on the calibration. Rather than performing a linear regression on the entire data set simultaneously, regressions are performed on each pair of data points. 30% of the data outliers are then removed and the mean of the relevant parameters taken.

### 3.3. Typical calibration curves

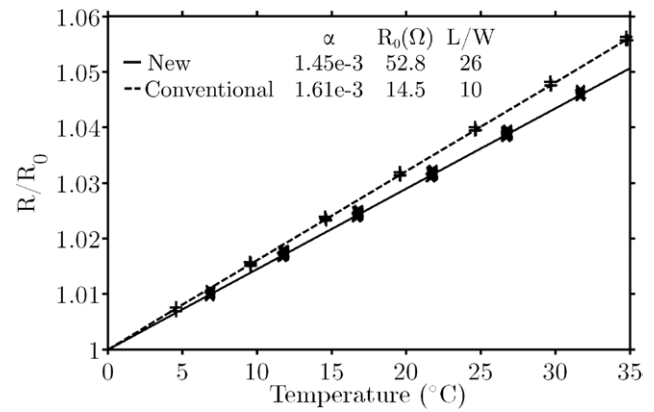
The calibration curves of typical conventional and new gauges are plotted in figure 10. Both of the calibrated  $\alpha$  values are significantly less than the bulk platinum material value  $\alpha = 3.279 \times 10^{-3}$ . This is due to thin film effects as discussed by Neugebauer and Webb [16], resulting from a reduction in the mean free path of the electrons within the film. This is supported by the observation that  $\alpha$  reduces with decreasing platinum thickness.

## 4. Demonstration in test facility

TFHFGs are typically employed for heat transfer measurements on short duration transient facilities. One such example is the Oxford Turbine Research Facility (OTRF), used to simulate the conditions in the high pressure stage of a typical civil aircraft gas turbine. As described by Chana *et al* [17], the facility is an engine-scale rotating turbine facility which replicates engine-representative conditions of Mach number, Reynolds number, and gas-to-wall temperature ratio.

The rotor casing is witness to the periodic passing of the rotor blade tips. This subjects the casing to large transient heat loads at a frequency of 10 kHz. This offers a good opportunity to demonstrate both the low and high speed capabilities of the gauges.

Heat transfer measurements have been made on the rotor casing of the OTRF by Chana and Jones [18]. As pictured in figure 11, this study utilised an array of 7 TFHFGs placed on a Perspex block with a gauge to gauge spacing of 4.2 mm.

**Figure 10.** Calibration of conventional and new Oxford TFHFGs using 110 measurement points.

Thorpe *et al* [7] presents comparable data on a different facility using laser ablated gauges with a gauge to gauge spacing of 1.85 mm. Gauges were placed on a macor block interfaced with a number of Peltier heat pumps, used to alter the wall temperature at the start of the run.

The current study utilises a high density array of the new Oxford TFHFGs with a gauge to gauge spacing of 0.8 mm. This permits an array of 88 TFHFGs in two parallel axial strips 35 mm wide as pictured in figure 11. Gauges were placed on an aluminium block incorporating a water circuit. Heated or cooled water is circulated to alter the wall temperature at the start of the run in a similar fashion to Thorpe *et al* [7]. This permits measurements over a wider range of measured wall temperatures which improves the regression to obtain the adiabatic wall temperature and heat transfer coefficient.

### 4.1. Experimental setup

The surface temperature history from a TFHFG is recorded by supplying each gauge with a constant current and measuring the voltage across it. The frequency response of TFHFGs reduces at high heat flux frequencies [12] and for high speed measurements (>1 kHz), a high-frequency amplifier is required to avoid digitisation errors in the high frequency part of the signal. At Oxford the TFHFG electronics and data acquisition systems have recently been upgraded. TFHFGs are now connected to a two break-point gain-shaping heat transfer amplifier (HTA) to boost the high frequency components of the temperature signal. The boosted output from the HTA is recorded by a high speed data acquisition system (DAQ) at a 2 MHz sampling frequency. The recorded signal is de-boosted in Matlab (which has much greater resolution than the DAQ) with an impulse response filter to recover the measured temperature signal. This can then be converted to heat-flux using the impulse method as described by Oldfield [6]. This method enables the measurement of signals with a bandwidth of approximately 150 kHz (limited by the thermal properties of the gauge). The work process for measuring and processing heat transfer data is summarised in figure 12.

The high speed boosted signal from the HTA is ac coupled, recording only the rise in wall temperature. To measure

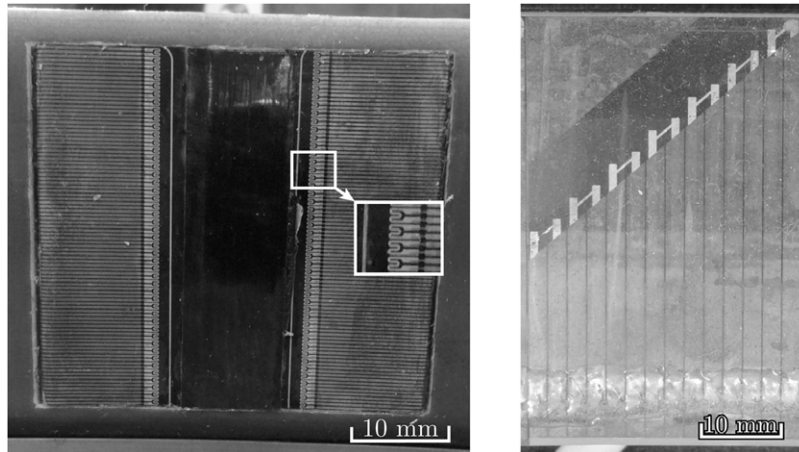


**Figure 11.** Casing instrumented with 88 TFHFGs as used in current study (left) and the 7 utilised by Chana and Jones [18] (right).

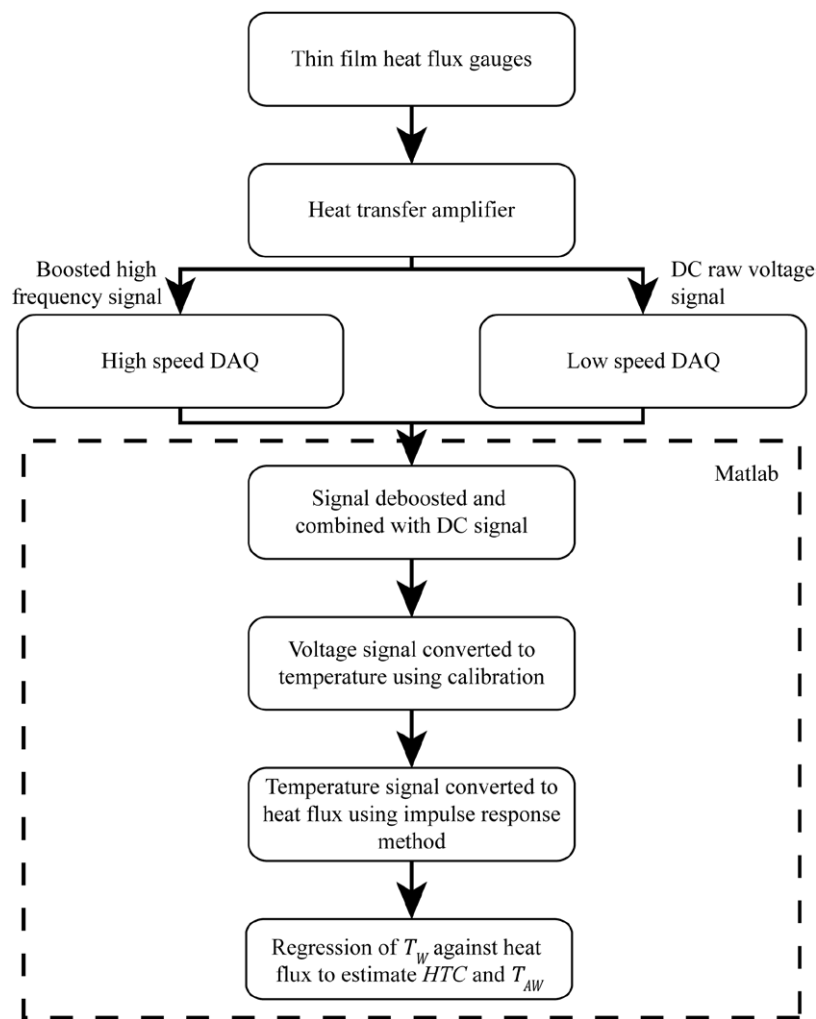


**Figure 12.** Work process for measuring, recording and processing heat transfer data.

absolute temperatures, the initial wall temperature must be known. If the instrumentation can be assumed to be isothermal immediately before the experiment, this can be measured using thermocouples placed under the TFHFGs. This is often not the case and the low speed dc signal must also be recorded and referenced to an earlier point when the instrumented region can be assumed to be isothermal.

The adiabatic wall temperature and heat transfer coefficient are typically found by performing a linear regression between the measured temperature ( $T_w$ ) and computed heat flux ( $\dot{q}$ ) to solve the convective heat flux equation, as described by Qureshi *et al* [19].

$$\dot{q} = -h(T_w - T_{AW}) \quad (10)$$



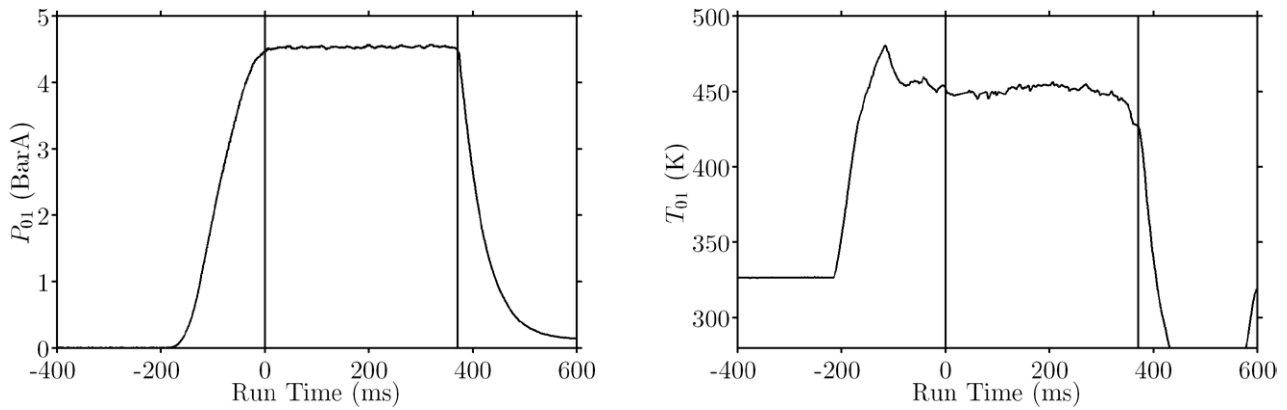


**Figure 13.** Plots of measured inlet total pressure (top) and inlet total temperature (bottom) for a typical OTRF run.

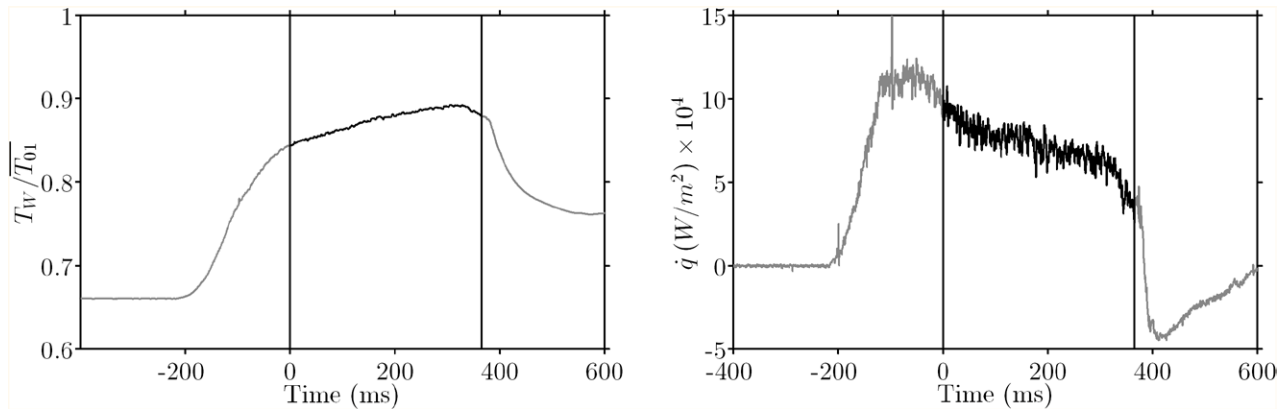


**Figure 14.** Plots of measured  $T_W$  (top) and  $\dot{q}$  calculated using impulse response (bottom) from a TFHFG during a run.

The intercept with the temperature axis (zero heat flux) corresponds to the adiabatic wall temperature and the slope ( $d\dot{q}/dT$ ) of the regression corresponds to the heat transfer coefficient. Use of the linear regression technique assumes that the local driving temperature ( $T_{AW}$ ) at the measurement location remains constant through the run.

#### 4.2. Experimental data

The OTRF presents several challenges to heat transfer processing. As evidenced in figure 13, though the inlet total pressure in the working section is very stable for the aerodynamically stable portion of the run, the inlet total temperature varies quite substantially. There is also a peak in total temperature before the start of the run which has a very negative effect on heat transfer processing, as much of the surface temperature rise on the instrumented wall occurs during this period.

Figure 14 shows the measured wall temperature and derived heat flux from a single TFHFG located on the HP rotor casing during a run with a 500 Hz low pass filter applied. The aerodynamically stable portion of the run is marked. The effect of the peak in inlet total temperature before the aerodynamically stable part of the run is clearly evident, resulting in a ~70 K rise in wall temperature before the run starts. The resulting small temperature rise which occurs during the stable portion of the run significantly increases the uncertainty in the results.

The ability to set the initial wall temperature over a number of runs using the water heater/cooler significantly expands the range of temperatures over which heat flux is recorded. Further data processing techniques can be applied to correct for changes in the local driving temperature, though these are beyond the scope of this paper.

#### 5. Conclusions

A new fabrication process for the manufacture of TFHFGs has been described and compared to previous methods. New gauge designs which improve the sensitivity for a given footprint are also introduced. The result is the ability to manufacture gauges which are both significantly smaller and more robust. Examples of TFHFGs which offer a 7 fold increase in gauge density are presented.

Methods for calibrating TFHFGs are discussed, with typical calibrations for both new and conventional TFHFGs compared. Calibrations performed in a new calibration facility are described and demonstrate that gauges manufactured using the conventional and new Oxford methods have comparable calibrations.

The work process for measuring, recording and processing heat transfer data on an experimental facility is described. The challenges of processing heat transfer data on a transient rotating facility are outlined and sample experimental data are presented.

## Acknowledgments

We would like to thank Rolls-Royce plc for funding this research.

## References

- [1] Vidal R J 1956 Model instrumentation techniques for heat transfer and force measurements in a hypersonic shock tunnel Cornell Aeronautical Laboratory, *Report AD-917-A-1*
- [2] Jones T V 1988 Gas turbine studies at Oxford 1969–1987 ASME 8-GT-112 *Presented at the Gas Turbine and Aeroengine Congress (Amsterdam, The Netherlands)*
- [3] Jones T V 1995 The thin film heat transfer gauges—a history and new developments *Invited Lecture, 4th National UK Heat Transfer Conf., IMechE Conf. Transaction (Manchester)* p 1–12
- [4] Schultz D L and Jones T V 1973 AGARD 165—Heat transfer measurements in short duration hypersonic facilities *Presented at Advisory Group for Aerospace Research and Development (Paris, France)* p 157
- [5] Doorly J E and Oldfield M L G 1986 The theory of advanced multi-layer thin film heat transfer gauges *Int. J. Heat Mass Transfer* **30** 1159–68
- [6] Oldfield M L 2008 Impulse response processing of transient heat transfer gauge signals *J. Turbomach.* **130** 021023
- [7] Thorpe S J, Yoshino S, Ainsworth R W and Harvey N W 2004 Improved fast-response heat transfer instrumentation for short-duration wind tunnels *Meas. Sci. Technol.* **15** 1897
- [8] Epstein A H, Guenette G R, Norton R J G and Yuzhang C 1986 High-frequency response heat-flux gauge *Rev. Sci. Instrum.* **57** 639–49
- [9] Anthony R J, Clark J P, Kennedy S W, Finnegan J M, Johnson D, Hendershot J and Downs J 2011 Flexible non-intrusive heat flux instrumentation for the AFRL research turbine *ASME Paper No. GT2011-46853*
- [10] Hodak M P 2010 Quantification of fourth generation kapton heat flux gauge calibration performance *Doctoral Dissertation* Ohio State University
- [11] Guo S M, Lai C C, Jones T V, Oldfield M L G, Lock G D and Rawlinson A J 1998 The application of thin-film technology to measure turbine-vane heat transfer and effectiveness in a film-cooled, engine-simulated environment *Int. J. Heat Fluid Flow* **19** 594–600
- [12] Anthony R J, Oldfield M L G, Jones T V and LaGraff J E 1999 Development of high density arrays of thin film heat transfer gauges *5th ASME/JSME Thermal Engineering Joint Conf. (San Diego, CA)* AJTE 99–6159
- [13] Chew M, Soon W H, Su N, Liao E, Rao V S, Premachandran C S, Kumar R and Damaruganath P 2009 Development of negative profile of dry film resist for metal lift off process *EPTC '09. 11th Electronics Packaging Technology Conf. 2009 (Singapore)* pp 884–8
- [14] Yang C H, Lee S C, Wu J M and Lin T C 2005 The properties of copper films deposited on polyimide by nitrogen and oxygen plasma pre-treatment *Appl. Surf. Sci.* **252** 1818–25
- [15] Piccini E, Guo S M and Jones T V 2000 The development of a new direct-heat-flux gauge for heat-transfer facilities *Meas. Sci. Technol.* **11** 342
- [16] Neugebauer C A and Webb M B 1962 Electrical conduction mechanism in ultrathin, evaporated metal films *J. Appl. Phys.* **33** 74–82
- [17] Chana K, Cardwell D and Jones T 2013 A review of the Oxford Turbine Research Facility *ASME Paper No. GT2013-95687*
- [18] Chana K S and Jones T V 2003 An investigation on turbine tip and shroud heat transfer *J. Turbomach.* **125** 513–20
- [19] Qureshi I, Smith A D, Chana K S and Povey T 2012 Effect of temperature nonuniformity on heat transfer in an unshrouded transonic HP turbine: an experimental and computational investigation *J. Turbomach.* **134** 011005